

A multi-objective evolutionary approach for integrating renewable energy in remote mines: A case study in Ellesmere Island (Nunavut, Canada)[#]

Daksh Khanna¹, Helen Li¹, Wania Khalid¹, Minghan Xu^{1*}

¹ Department of Civil and Mineral Engineering, University of Toronto, Toronto, ON M5S 1A4, Canada

(*Corresponding Author: minghan.xu@utoronto.ca)

ABSTRACT

This paper develops a novel multi-objective optimization framework, capable of predicting the optimization of renewable energy integration from available sources in northern and remote regions, while considering energy supply, cost, greenhouse gas emissions (GHG), and social impacts. Wind turbines, photovoltaic (PV) panels, small modular reactors (SMRs), and geothermal systems, along with lithium-ion batteries, are modeled separately. Multi-objective evolutionary algorithms (MOEAs) are employed to systematically evaluate each technology from energy and cost to environmental and social impacts. Applied to Ellesmere Island, the optimal renewable deployment halves cost (\$500M in lifetime savings), reduces carbon emissions by over 90%, and eases social disagreement from 53% to 36% compared to diesel grids. The solution is viable, provided a payback period of less than 6 years to recoup the higher initial capital costs.

Keywords: Advanced energy systems, multi-objective optimization, evolutionary algorithms, renewable energy, sustainable mining, Northern Canada.

1. INTRODUCTION

Driven by today's global energy transition, the demand for critical minerals is higher than ever before, as these resources are essential for renewable energy technologies (e.g., solar panels and wind turbines) and energy storage systems (e.g., batteries) [1]. However, realizing this potential requires a significant ramp-up in mining activities, particularly in Canada's North, where 23 out of 31 critical minerals are abundantly found [2]. Canada's North is vital to the country's economic growth but faces major challenges due to its reliance on fossil fuels. These regions also represent some of Canada's most socially and environmentally sensitive areas, as they are home to many Indigenous and First Nations communities [3]. Thus, the sustainable development of

mining in Canada's North requires consideration not only of its energy sources and economic benefits but also of its environmental and social impacts.

The literature on renewable energy integration for northern mining operations emphasizes the techno-economic analysis for a single or two energy sources that quantifies the feasibility of mine decarbonization. Tardy et al. [4] evaluate the feasibility of decarbonizing the Raglan mining site in northern Quebec by integrating wind power with pumped hydro storage, modeled under variable wind speeds and extreme climatic conditions. Their results show that the hybrid system can reduce diesel use by 52.2% and deliver long-term cost savings with an estimated 11-year payback period. Bayomy et al. [5] are among the few to investigate multiple renewable energy sources and storage systems. Their nuclear renewable hybrid energy system (NR-HES), including small modular reactors, wind turbines, molten salt storage, hydrogen storage, and peaking diesel generators, is studied for the Victor mine site in northern Ontario. The optimization result indicates a feasible near-zero-emission operation, with greenhouse gas (GHG) emissions reduced by up to 94.8% and minimal increases in annualized costs when prioritizing environmental and economic objectives. Notably, a recent review by Arasteh et al. [6] examines strategies to reduce diesel reliance in off-grid Indigenous communities in Northern Quebec, covering a wide range of renewable options such as hydropower, wind, solar, geothermal, and biomass. They highlight the importance of successful case studies and the integration of Indigenous knowledge for achieving a sustainable and culturally appropriate energy transition.

Current literature for renewable mine energy systems is not without gaps. While techno-economic assessment with the potential of reducing GHG emissions has been conducted for selected energy sources, there has not been a study that combines them

[#] This is a paper for the 17th International Conference on Applied Energy (ICAE2025), December 8-12, 2025, Bangkok, Thailand.

with their social impacts and optimizes all available renewable sources in Northern Canada. In this work, we present a novel framework that evaluates wind, solar, nuclear, and geothermal power with lithium-ion (Li-ion) battery storage; economic benefits, GHG emissions, and social impacts are considered for each technology and optimized through multi-objective evolutionary algorithms (MOEAs). Moreover, a case study is performed in Ellesmere Island (Nunavut), an off-grid region in Canada's North.

2. METHODOLOGY

2.1 Overview of MOEA framework

To develop an ideal set of renewable technologies for a remote location, the technologies are optimized on a multi-level process: the first level optimizes wind and geothermal technologies for levelized cost of energy (LCOE) based on site conditions (wind speed, ambient temperature, ground temperature), and the second step finds the non-dominated set of wind, solar, nuclear, and geothermal for LCOE, emissions intensity (CI), and social disagreement (SD). The first level is optimized using the Differential Evolution (DE) algorithm as it is robust on multimodal landscapes and easy to parallelize (independent candidate evaluations). The applied variation of the algorithm is as follows [7, 8]:

- 1) Draw initial population using Latin hypercube sampling (LHS).
- 2) Evaluate candidate solution x_i for LCOE and physical feasibility constraints.
- 3) Terminate if the design-space tolerance criterion is met.
- 4) If not, mutate x_i ; sample distinct indices to build donor $v_i = x_{\pi_1} + F(x_{\pi_2} - x_{\pi_3})$.
- 5) Combine (v_i, x_i) via binomial crossover to build trial u_i .
- 6) Take better of (x_i, u_i) and repeat till termination.

From here, the optimized technologies are reoptimized for the problem formulation:

- The decision variables: number of turbines, area of solar grid (km^2), number of geothermal plants, and power rating of SMR
- The objectives are: $f_1 = \text{LCOE}$, $f_2 = \text{CI}$, and $f_3 = \text{SD}$
- The problem is constrained as:
 - $g_1 = -\min_m(G_m - D_m)$, where (G_m, D_m) are grid generation and mine demand, respectively.
 - $g_2 = \text{LCOE}_{\text{grid}} \leq \text{LCOE}_{\text{diesel}}$.

The problem is solved using the non-dominated sorting genetic algorithm (NSGA-II) following the steps demonstrated in Figure 1:

- The population is seeded with extreme-point solutions and then filled with LHS.
- The generations are evaluated as a set X on $F = [f_1, f_2, f_3]$ and $G = [g_1, g_2]$.
- The mating pool is constructed using binary tournament selection. Solutions are sampled (with replacement) to take those with a lower

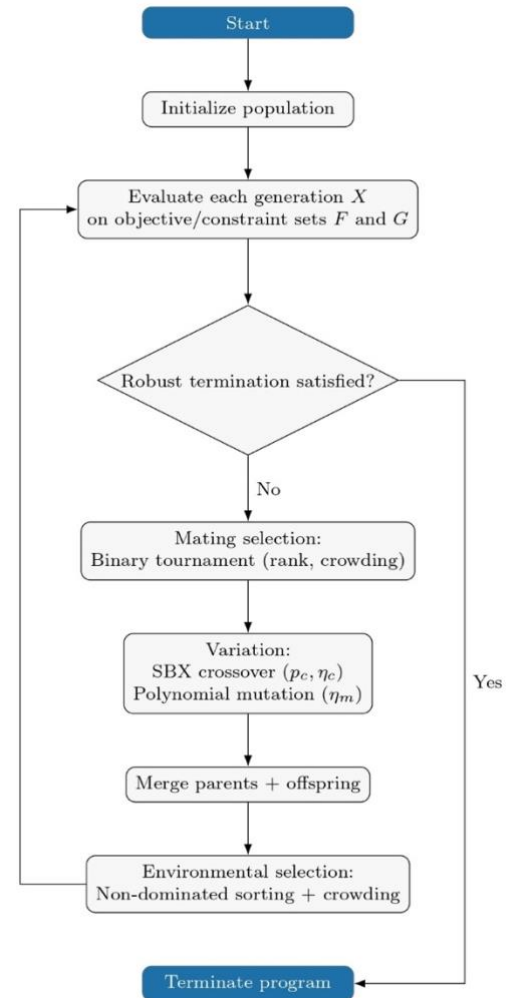


Figure 1. Flowchart representation of NSGA-II.

- non-dominated rank (crowding distance for ties)
- The offspring are generated through simulated binary crossover (SBX), mixing decision variables from parents and mutating using polynomial mutation (bounds repaired as needed).
- The next generation is formed using environmental selection. Parent and offspring generations are combined to fill fronts sorted by non-dominated ranking and crowding distance.

2.2 Energy modeling

The wind power generation is predicted by a turbine model based on a large (>1 MW) horizontal-axis wind turbine. This is representative of those commonly deployed in utility-scale power grids [9]. The electrical power of a wind turbine, P_{wind} , can be described as:

$$P_{\text{wind}} = \frac{1}{2} \rho A v_{\text{wind}}^3 c_{\text{wind}} \eta_{\text{wind}}$$

where $\rho, A, v_{\text{wind}}, c_{\text{wind}}, \eta_{\text{dt}}$ are the air density, rotor area, wind velocity, power coefficient that is the fraction of wind power converted into mechanical power at the turbine shaft, and drivetrain (gearbox + generator) efficiency which is treated as a constant (fixed at 95% [10]), respectively. Moreover, the wind turbines are simulated across four operational regions defined by wind speed: (i) below cut-in, (ii) between cut-in and rated, (iii) between rated and cut-out, and (iv) above cut-out. Power output is constant in regions (i), (iii), and (iv), while the non-rated region (ii) is modeled explicitly. In region (ii), turbine performance depends on the power coefficient c_{wind} which varies with turbine type and rating and is fitted to NREL turbine performance data with an absolute RMSE of 0.14%.

The energy generated by a PV module can be evaluated by the following equation [11]:

$$P_{\text{solar}} = G A_{\text{PV}} \eta_{\text{solar}}$$

where $G, A_{\text{PV}}, \eta_{\text{PV}}$ are the solar irradiation, area of the PV modules, and the efficiency of solar power calculated by the wire (assumed to be 99% [12]), the inverter (which is fixed at 95.5% [12]), and the PV module itself. The efficiency of the module is dependent on its temperature given by [11]:

$$\eta_{\text{PV}} = \eta_0 \times [1 + \gamma(T_{\text{PV}} - 25)]$$

where η_0 and γ are the efficiency at standard conditions and the temperature coefficient that represents how much the efficiency changes per °C. These values depend on the brand of PV module; for example, a LONGi PV module has the standard efficiency of 22.7% and temperature coefficient of $-0.28\%/^{\circ}\text{C}$. In addition, the PV module's temperature is a function of the air temperature and solar irradiation according to Khatib's model [11].

For SMR, a pressured water reactor (PWR) is utilized; a fuel-burnup model is used [13] and is expressed as:

$$P_{\text{nuclear}} = \frac{m \times B \times \eta_{\text{nuclear}}}{t_{\text{day}}} \times 10^6$$

where $m, B, \eta_{\text{nuclear}}, t_{\text{day}}$ are the uranium's mass in the fuel, burnup (i.e., the amount of energy released per kg of uranium), thermal efficiency of the reactor, and refueling cycle in days, respectively. It is noted that the fuel burnup determines how much fuel is needed and how often fuel needs to be replaced [14]. For PWRs, the burnup ranges from 20–65 MWd/kg, and the time before refueling is between 1–4 years [15].

For extracting and electrifying geothermal heat, a binary geothermal plant is modeled using a subcritical Organic Rankine Cycle (ORC) with an air-cooled condenser (ACC), where produced brine transfers heat to a closed working-fluid loop and is re-injected via a production-injection doublet. The ORC is modeled as a four-state cycle, i.e., pressurization, heating, turbine expansion, and condensation, with thermophysical properties evaluated using CoolProp [16]. The electrical power can be calculated as [17]:

$$P_{\text{geo}} = P_{\text{gross}} - (P_{\text{pump}} + P_{\text{ACC}})$$

where $P_{\text{gross}}, P_{\text{pump}}, P_{\text{ACC}}$ are the gross electric power (i.e., working-fluid mass flow multiplied by total work done in the ORC), pumping power (i.e., required to pump the production and injection wells), and power required to run the ACC that can cool down rejected heat from the working fluid.

Due to the intermittent nature of wind and solar power generation (e.g., low wind speeds and cloudy conditions), a storage system is required. Here, a utility-scale Li-ion battery with Lithium Iron Phosphate (LFP) chemistry is modeled for short-duration curve smoothing, using simplified performance and replacement logic to minimize costs [18]. The energy stored at its maximum charge by Li-ion battery is given by $E_{\text{battery}} = P_{\text{rated}} \times t_{\text{hour}}$, where P_{rated} and t_{hour} are the rated power of the battery and the number of hours that the battery can operate at its rated power.

2.3 Cost modeling

The LCOE for wind, solar, nuclear, and geothermal energy systems is calculated using NREL recommendations from [19]:

$$\text{LCOE} = \frac{C_{\text{ICC}} \times \text{CRF} + C_{\text{O\&M}}}{\text{AEP}}$$

where C_{ICC} is the initial capital cost, $C_{O\&M}$ is the yearly operations and maintenance cost ($C_{O\&M} = C_{O\&M, \text{fixed}} + C_{O\&M, \text{variable}}$), and CRF is the capital recovery factor, found as:

$$CRF = \frac{[i(i+1)^n]}{[(i+1)^n - 1]}$$

Here, i is the discount rate (an average of 7.18% for mining projects [20]), and n is the project lifetime.

The initial capital cost for the wind turbines is adopted from Chen et al.'s model [21], which includes both the turbine system cost (e.g., mechanical, electrical, electronic) and the balance of the station cost (e.g., infrastructure, installation, transportation). As for the PV system, the capital cost is primarily influenced by the installation cost of solar panels expressed as [22]:

$$C_{ICC, \text{solar}} = G_0 \eta_0 C_{\text{watt}}$$

where C_{watt} is the cost per Watt that can be assumed to be \$1.27/W for utility scale PV systems [23]. Moreover, a standard 20Mwe SMR has a capital cost \$9,502.06/kW [24], and the initial cost of geothermal system includes the prices of drilling [25], well [26], and ORC [27]. Regarding the cost of storage systems (i.e., Li-ion battery), a different cost model was proposed where the total cost is the summation of capital expenditures (CAPEX) and operations and maintenance (O&M). This model is adopted from PNNL's newest dataset [18].

2.4 Environmental impact

The environmental impact of each technology is assessed through its emission intensity (CI), defined as the GHG emissions associated with manufacturing, operation, and decommissioning, expressed in grams of $\text{CO}_{2, \text{eq}}/\text{kWh}$.

Turbine emissions are derived using Padey's simplified life cycle assessment (LCA) of 17 onshore wind turbines [28]. Emission intensity is interpolated bilinearly across wind speed and turbine lifetime, while the mean wind speed is calculated from Weibull parameters. Solar emissions are based on LCA of utility-scale PV with module, installation, O&M, and end-of-life carbon footprints [29]. While the nuclear emissions are based on Warner and Heath's LCA of 99 light-water reactors (LWRs), including the upstream, operational, and downstream emissions [30]. The geothermal emissions are modelled using Lacirignola's LCA framework, considering contributions from well drilling, brine

pumping, and ORC operations [31]. The total emissions of Li-ion batteries consider the rated capacity, number of battery units, and life-cycle intensity (e.g., project lifetime, depth of discharge, and round-trip efficiency) [32].

2.5 Social impact

Social impact is defined as the extent to which a community is willing to host a given energy generation technology. This metric is built using polling data, under the assumption that more favorable polling results correspond to higher acceptance, a more readily attainable social license to operate (SLO), and a less complex permitting process.

The overall grid acceptance is found as the energy-weighted average acceptance across all technologies:

$$S_{\text{grid}} = \frac{\sum_{n=1}^N S_n E_n}{\sum_{n=1}^N S_n}$$

where S_n denotes the social acceptance parameter of technology n and E_n is the annual electricity contribution to the grid. Hence, the grid disagreement is given by $SD_{\text{grid}} = (1 - S_{\text{grid}}) \times 100\%$. The acceptance parameter is listed in Table 1.

Table 1. Polling-based acceptance parameters used in the social impact model.

Technology	S_n	Confidence Interval	Time of Fieldwork	Ref.
Wind	0.86	$\pm 2.5\%$	2023/10	[33]
Solar	0.90	$\pm 2.5\%$	2023/10	[33]
Nuclear	0.51	$\pm 2.5\%$	2023/10	[33]
Geothermal	0.67	$\pm 2.6\%$	2013/11	[34]
Diesel	0.47	$\pm 1.89\%$	2024/11	[35]

3. RESULTS AND DISCUSSION

The case study is performed at Ellesmere Island, Nunavut, Canada ($79^\circ 50' \text{N}$, $78^\circ 00' \text{W}$). After the first level of optimization, the ideal technologies based on site conditions are given by Table 2 and 3 for wind turbines and the geothermal plant, respectively.

Table 2. The first-level optimization of wind turbines.

Metric	Value
Radius (m)	46
Rated power (kW)	1,476
Hub height (m)	126
LCOE (USD/kWh)	0.0705
Annual energy (kWh)	4,119,959
Annual cost (USD)	40,228

Initial capital cost (USD)	3,047,608
Emissions intensity (g CO _{2,eq} /kWh)	14.0

Table 3. The first-level optimization for the geothermal plant.

Metric	Value
Ideal fluid	Butane
Ideal depth	4,953
Ideal flow rate	200
LCOE (USD/kWh)	0.1759
Annual energy (kWh)	26,726,031
Annual cost (USD)	822,721
Initial capital cost (USD)	47,257,187
Emissions intensity (g CO _{2,eq} /kWh)	25.4

The second level is optimized with ideal technologies to produce the Pareto Front (non-dominated solutions) as shown in Figure 2. The nuclear power dominates LCOE, while wind dominates CI and SD. It is valuable to note that while wind technology on its own is cost effective, the batteries needed for it make it a worse LCOE solution than nuclear. Geothermal performs best in lower SD regions as a fixed technology to offset battery use. Solar is an unfeasible solution under constraint g_2 ; however, it would perform the best on SD if the solutions were constrained to those more economic than diesel grids.

A single solution can be taken off the Pareto front to demonstrate a potential solution for off-grid location, as listed in Table. This solution is adopted using the weighting $F = [0.7, 0.1, 0.2]$ with the weighted sum model (WSM). The demand this solution meets is based on the Diavik Diamond Mine’s energy demands [36]. The lifetime savings for the renewable grid is listed in Table 4. Figure 3 shows the renewable grid’s payback period and savings over project lifetime. It is clear to observe

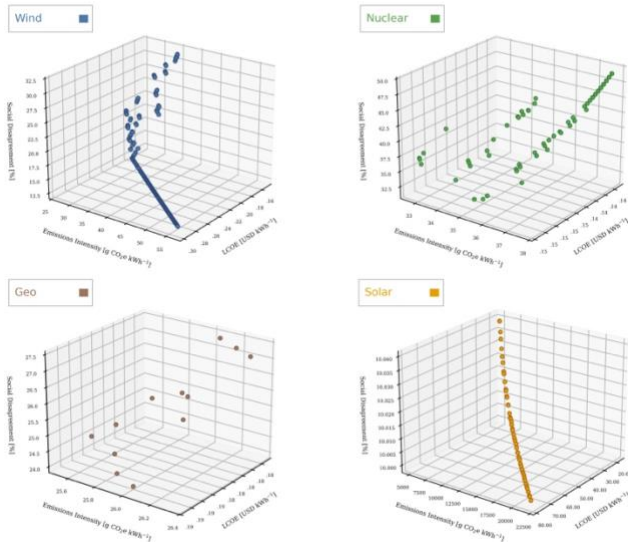


Figure 2. Pareto fronts (separated by technology).

that the optimal renewable grid will reach the cost level of the diesel grid within 6 years of the mining operation. The rate of increase in cost is also expected to be much lower in renewables compared with diesel machinery, with around a 20% increase over a 30-year operation.

Table 4. Renewable grid and diesel baseline performance on all objectives.

Metric	Value
LCOE (USD/kWh)	0.1447
Emissions intensity (gCO _{2,eq} /kwh)	35.58
Social disagreement (%)	35.57
Annual generation (kWh/yr)	258,039,586
Mine Demand (kWh)	206,000,000
Wind (%)	38.30
Solar (%)	0.00
Geothermal (%)	0.00
SMR (%)	61.60
Initial capital cost (USD)	288,722,137.42
Annual O&M total (USD/yr)	6,217,094.09
Total annual emissions (gCO _{2,eq} /yr)	7,355,136,770
Battery rating (kW)	3,421.07
Battery duration (h)	10.98
Battery energy capacity (MWh)	37.55
Diesel Initial Capital Cost (USD)	19,631,780.82
Diesel annual O&M (USD/kWh)	59,447,787.40
Diesel emissions intensity (gCO _{2,eq} /kwh)	804.9
Diesel LCOE (USD/kWh)	0.2954

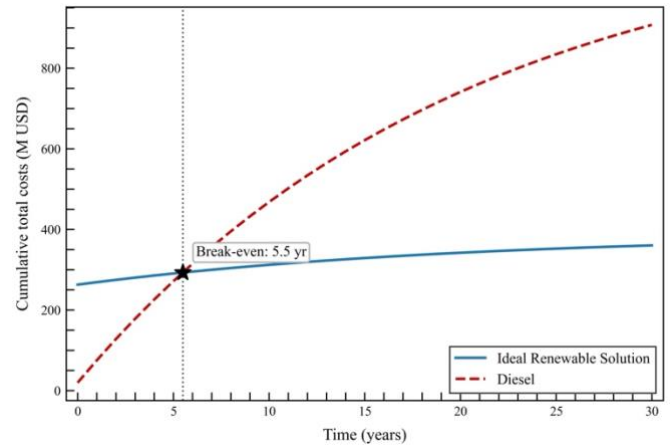


Figure 3. Cost trajectories of renewable and diesel grid in present value.

4. CONCLUSION AND FUTURE WORK

This work introduced a two-stage MOEA framework that tailors wind and geothermal technologies to local resource conditions and optimizes a system-level mix for cost (LCOE), life-cycle carbon emissions (CI), and a

polling-based social impact metric via DE and NSGA-II. Applied to Ellesmere Island, the framework yields a set of non-dominated solutions, where nuclear and wind dominate the three objectives. Geothermal improves social disagreement solutions by offsetting storage needs, and solar is infeasible under the technoeconomic constraints. A representative configuration achieves an LCOE of 0.1447 USD/kWh (50% lower than the diesel baseline) and with over 90% lower emissions intensity. The results indicate that site-optimized renewable configurations can displace diesel as the primary energy source in remote mines. For future work, the framework could be benefited from including more case studies, incorporating hourly dispatch with variable demand, refining the social metric using region-specific data, and performing sensitivity tests to account for uncertainty.

REFERENCE

- [1] S. Carr-Wilson, S. K. Pattanayak, and E. Weinthal, "Critical mineral mining in the energy transition," *Energy Res. Soc. Sci.*, vol. 116, 2024, Art. 103672.
- [2] Mining Association of Canada, *The Mining Story 2024: Canadian Mining Industry Facts and Figures*, 2024.
- [3] T. D. Pearce *et al.*, "Climate change and mining in Canada," *Mitig. Adapt. Strateg. Glob. Change*, vol. 16, no. 3, pp. 347–368, 2011.
- [4] A. Tardy *et al.*, "Enhancing energy sustainability ... Raglan Mine," *Energies*, vol. 18, no. 9, 2025, Art. 2184.
- [5] A. M. Bayomy *et al.*, "Small modular reactors for green remote mining," *Energy Convers. Manag.: X*, vol. 19, 2023, Art. 100397.
- [6] H. Arasteh *et al.*, "Decarbonization strategies for Northern Quebec," *Energies*, vol. 18, 2025, Art. 4234.
- [7] M. F. Ahmad *et al.*, "Differential evolution: A recent review," *Alexandria Eng. J.*, vol. 61, no. 5, pp. 3831–3872, 2022.
- [8] J. Blank and K. Deb, "pymoo: Multi-Objective Optimization in Python," *IEEE Access*, vol. 8, pp. 89497–89509, 2020.
- [9] L. M. Sheridan *et al.*, *Distributed Wind Market Report: 2024 Ed.*, PNNL, 2024. (PNNL-36057).
- [10] Y. Guo *et al.*, "Three- vs four-point drivetrain configurations," *Wind Energy*, vol. 20, no. 3, pp. 537–550, 2017.
- [11] T. Khatib, "Optimization of a grid-connected renewable energy system," *Int. J. Low-Carbon Technol.*, vol. 9, no. 4, pp. 311–318, 2014.
- [12] E. Ghiani, F. Pilo, and S. Cossu, "On the performance ratio of photovoltaic installations," in *Proc. IEEE Grenoble Conf.*, 2013, pp. 1–6.
- [13] E. V. Semenov and V. V. Kharitonov, "Burnup vs. enrichment of prospective fuel," *Nucl. Energy Technol.*, vol. 9, no. 4, pp. 239–244, 2023.
- [14] Z. Xu, *Design Strategies for Optimizing High Burnup Fuel in PWRs*, Ph.D. diss., MIT, 2003.
- [15] IAEA, *Small Modular Reactor Technology Catalogue: 2024 Ed.*, 2024.
- [16] I. H. Bell *et al.*, "CoolProp," *Ind. Eng. Chem. Res.*, vol. 53, no. 6, pp. 2498–2508, 2014.
- [17] Idaho National Laboratory, *GETEM User Manual*, INL/EXT-16-38751, 2016.
- [18] PNNL, *Lithium-ion Battery Cost & Performance Database*, 2024.
- [19] NREL, *Simple LCOE Calculator Documentation*, 2025.
- [20] A. Ovalle, "Analysis of the discount rate for mining projects," in *MassMin 2020*, 2020, pp. 1048–1064.
- [21] J. Chen, F. Wang, and K. A. Stelson, "Minimizing cost of energy for large utility wind turbines," *Appl. Energy*, vol. 228, pp. 1413–1422, 2018.
- [22] M. Sodhi *et al.*, "Economic lifetimes of solar panels," *Procedia CIRP*, vol. 105, pp. 782–787, 2022.
- [23] D. Feldman *et al.*, *Spring 2024 Solar Industry Update*, NREL, 2025.
- [24] N. Butcher *et al.*, *SMR Roadmap: Economic and Finance Working Group*, 2018.
- [25] D. Akindipe and E. Witter, *Geothermal Drilling Cost Curves Update*, 2025.
- [26] J. W. Tester *et al.*, *The Future of Geothermal Energy—Impact of Enhanced Geothermal Systems (EGS) on the United States in the 21st Century*, MIT, Cambridge, MA, USA, 2006.
- [27] S. Lemmens, "Cost estimation of organic Rankine cycle systems," *Energies*, vol. 9, no. 7, p. 485, 2016.
- [28] P. Padey *et al.*, "Simplified LCA for wind electricity," *J. Ind. Ecol.*, vol. 16, pp. S28–S38, 2012.
- [29] B. L. Smith *et al.*, *Updated LCA of Utility-Scale PV in the U.S.*, NREL, 2024.
- [30] E. S. Warner and G. A. Heath, "LCA of nuclear electricity generation," *J. Ind. Ecol.*, vol. 16, pp. S73–S92, 2012.
- [31] M. Lacirignola *et al.*, "Life-cycle GHG of enhanced geothermal systems," *Geotherm. Energy*, vol. 2, p. 8, 2014.
- [32] D. Y. Lee *et al.*, *Potential GHG Reductions from Plug-in EVs*, NREL, 2024.
- [33] M. Hrobsky, *Public Opinion About Electricity Generation*, Ipsos, 2023.
- [34] A. Friser *et al.*, *The Social Acceptability of Geothermal Energy*, in *Geothermal Energy and Society*, Springer, 2025, pp. 119–140.
- [35] ABACUS Data, *Environmental Defence: Public Opinion Survey*, 2024.
- [36] ACAP, "Diavik Wind Farm, Yellowknife, Canada," Arctic Council, accessed Sep. 18, 2025.